Modelling and Analysis of the Operational Characteristics of Vanadium Redox Flow Battery

Xudong WANG, Shengtie WANG

College of Energy and Power Engineering, Inner Mongolia University of Technology, Hohhot, , 010051, China

***Abstract* — Vanadium redox flow battery (VRB) is a new type of battery energy storage system (BESS), which can be used in wind farms for: i) smoothing power output, ii) improving he low voltage ride through (LVRT) capability and iii) provide power grid stability. In this paper we analyze the electrochemical reaction mechanism and principles of VRB, and propose a new type of equivalent circuit model, in which the internal impedance and spurious impedance are taken into account. As a result, this model not only accurately represents the input and output characteristics, state of charge (SOC) and transient features, but also is easy to implement in terms of engineering. The simulation model of VRB is established in Matlab platform, and its operation characteristics analysis is done under the constant current mode (CCM), constant power mode (CPM) and variable current mode (VCM). The mathematical model between VRB battery efficiency and charge-discharge current is put forward for the first time, and the effects of transient features and temperature on the battery performance are analyzed. The simulation results show that VRB has excellent steady and transient features and verifies the correctness of the equivalent circuit model and simulation model. The work done in this paper lays good theoretical foundation for further study of the VRB energy storage system (VRB-ESS).**

Keywords - vanadium redox flow battery (VRB); wind power generation; battery energy storage system (BESS); equivalent circuit; operation characteristic

I. INTRODUCTION

With the development of economy, the contradiction between energy demand and environmental pollution is becoming more and more prominent. As a kind of clean, environmentally friendly renewable energy, wind energy industry in China and other countries is developing rapidly, becoming the most effective way to solve the current environmental pollution and energy crisis[1]. Because of the randomness and volatility of wind speed, the output power of the wind power system changes with the wind speed, and the grid will have a negative impact on the stability and economy of the power system[2][3][4]. At present, the large scale wind farm connected to the grid needs to solve two major problems: 1) improving the low voltage ride through capability of the unit; 2) smoothing the output power of the wind farm.

The development of energy storage technology provides an effective way to improve the performance of wind power generation, improve the performance of wind power system and improve the controllability of wind farm output power [5][6][7]. Energy storage technology can not only smooth active power fluctuations, but also can adjust the reactive power, which can effectively solve the random and volatility of wind power. In addition, it also has the function of cutting the peak to fill the valley, saving energy and ensuring the safety of power system[8]. Energy storage technology mainly includes the physical storage, electromagnetic energy storage and electrochemical energy storage[9].

The vanadium redox flow batteries is well suited for applications of large-scale power energy storage, because of its large capacity, long life, low maintenance requirements, and rapid response etc. In recent years, many scholars have studied and explored the modeling of the vanadium redox flow battery. The open circuit voltage model of the VRB in the open circuit self discharge is established in[10], but the model error is caused by the neglect of the equilibrium of the electrolyte. In [11], the equivalent circuit of the VRB in the DC circuit is studied, and the influence of high frequency inductance is neglected, but the physical meaning of the model is not very clear. The mechanism model of the two dimensional single phase transient isothermal model is proposed in [12]. But it is not conducive to the simulation study due to large calculation.

The above modeling methods only studied the model structure under the action of a single variable, and the model's accuracy and rationality were affected by the assumption that the model parameters were not reasonable. A new model structure considering both the accuracy and the complexity is proposed in this paper, the operating characteristics and the influence of operating parameters on the performance of the model in different modes are analyzed.

II. OPERATING PRINCIPLE OF THE VRB

The main components of VRB include: electric reactor, electrolyte storage tank, power pump and cooling device, etc. The electric reactor is the core component of the whole battery device, which is composed of a series of single batteries, and adopts a closed lock structure. The electric reactor is divided into positive and negative electrode by ion exchange membrane, the positive electrode is V^{4+}/V^{5+} and the negative electrode is V^{2+}/V^{3+}. The electrolyte is composed of vanadium material and sulfuric acid, which are stored in the positive and negative liquid storage tank respectively. The positive and negative electrode is

transported by the power pump, the reaction is carried out on the graphite felt electrode, and the electric current of the bipolar plate is collected through the graphite sheet metal gate[13]. The operating principle of the VRB is illustrated in Fig. 1.

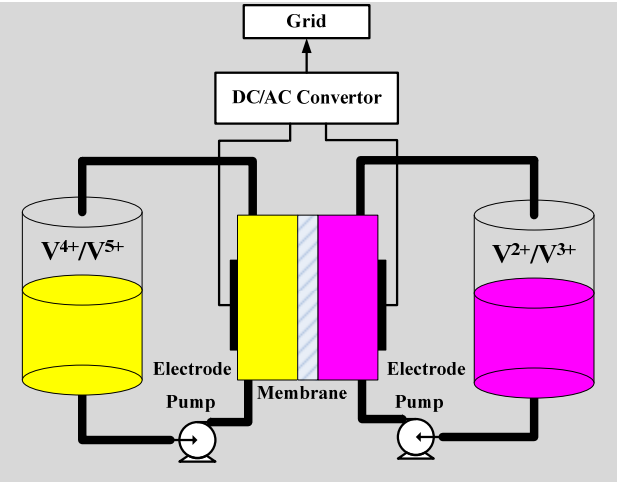

Figure 1. VRB operating principle.

Total power available is related to electrode area of the cell and total energy stored in VRB, which depends on both SOC and amount of active chemical substances. Simplified electrode reaction processes are as follows:

(1) For positive electrode, it is

$$V^{4+} - e^{-} \underset{\text{Discharge}}{\overset{\text{Charge}}{\rightleftharpoons}} V^{5+}$$

(2) For negative electrode, it is

$$V^{3+} + e^{-} \underset{\text{Discharge}}{\overset{\text{Charge}}{\rightleftharpoons}} V^{2+}$$

In the charging process, the blue V^{4+} ions are oxidized to yellow V^{5+} ions at the positive electrode surface, while the e^{-} are released, and the electronics are transmitted to the outer circuit through the electrode. The green V^{3+} ions are obtained from the external circuit, and the surface of the negative electrode are reduced to purple V^{2+} ions. The H^{+} ions in the positive electrode are transferred to the anode and the excess charge through the cation exchange membrane to maintain the neutral of the solution. In the discharging process , the H^{+} ions are transferred from the cathode to the positive electrode.

III. VRB MODELING

A. Equivalent circuit

Considering the physical and mathematical properties of the VRB, the equivalent circuit is shown in Fig. 2.

The VRB model uses the following equivalent method: 1) the stack voltage of the battery U_{stack} is affected by the charge state and the battery voltage of the battery, and it is simulated by a controlled voltage source; 2) SOC represents the number of active chemical substances, which is equivalent to a dynamic update variable; 3) the numerical value of the pump loss is related to the battery stack current I_{stack} and SOC, and it is simulated by a controlled current source; 4) equivalent resistance loss expressed as reaction resistance $R_{reaction}$ and ohmic resistance $R_{resistive}$; 5) the external parasitic resistance loss includes fixed resistor R_{fixed} and pump loss I_{pump}; 6) the dynamic response capability of the battery is indicated by the electrode capacity $C_{electrode}$.

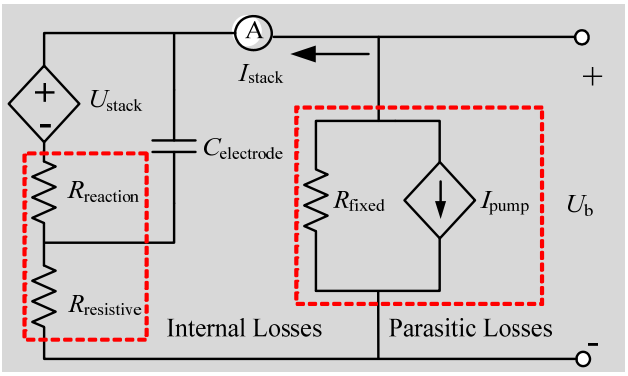

Figure 2. Equivalent circuit model of VRB.

B. Mathematical model

The calculations VRB parameters are based on estimating losses of 21% (15 % internal losses +6% parasitic losses) in the worse case operating point, for a minimum voltage of 42V, and a current of 95A.

1) Battery terminal voltage

Battery cell EMF cell U_{cell} correlates directly with SOC, according to the Nerst equation, expression is as following

$$U_{cell} = E + \frac{2RT}{F}\ln\left(\frac{SOC}{1-SOC}\right) \quad (1)$$

E is normal cell EMF，T is thermodynamic temperature(K), R is Molar gas constant(R=8.314J/(K·mol)), F is Faraday constant(F=96500C/mol).

The battery stack EMF of n cells in series

$$U_{stack} = nU_{cell} \quad (2)$$

The stack is modeled as a controlled voltage source, from expression(1)(2), it is known that the controlled voltage is mainly determined by the number of battery cells in series and SOC. The battery terminal voltage finally can be expressed as following

$$U_b = U_{stack} - I_{stack}(R_{reaction} + R_{resistive}) \quad (3)$$

2) Equivalent internal resistance

Equivalent internal resistance includes $R_{reaction}$ and $R_{resistive}$, their values can be estimated by power losses due to internal resistance at maximum discharge current I_{max}, generally they keep constant during overall battery operation period. Assuming that the power losses caused by $R_{reaction}$ and $R_{resistive}$ are 9 % , 6% of battery stack power P_{stack} separately, then

$$R_{\text{reaction}} = \frac{9\% \times P_{\text{stack}}}{I_{\max}^2}$$
$$R_{\text{resistive}} = \frac{6\% \times P_{\text{stack}}}{I_{\max}^2} \quad (4)$$

3) Parasitic power losses

Parasitic power losses includes fixed power loss modeled as fixed resistance R_{fixed} and variable power loss modeled as controlled current source I_{pump} , then

$$P_{\text{stack}} = \frac{P_{\text{rating}}}{1-21\%} \quad (5)$$

P_{rating} is the battery rated power, then

$$R_{\text{fixed}} = \frac{U_{\text{stack}}^2}{2\% \times P_{\text{stack}}}$$
$$I_{\text{pump}} = 1.011\frac{I_{\text{stack}}}{SOC} \quad (6)$$

4) Electrode capacitor

By measuring battery cell capacitor, the total electrode capacitor $C_{\text{electrode}}$ can be estimated according to the connection type of cells, then

$$C_{\text{electrode}} = \frac{6}{n} \quad (7)$$

5) SOC

SOC value can be forecasted precisely by chemical method in practical application. Here refer to Ampere-hour method, neglecting the effect of charge-discharge current on the actual total capacity, SOC is updated periodically by accumulating electrical energy flowing through the battery stack.

$$SOC(k+1) = SOC(k) + \Delta SOC$$
$$\Delta SOC = \frac{I_{\text{stack}} \times U_{\text{stack}} \times T_{\text{step}}}{P_{\text{rating}} \times T_{\text{rating}}} \quad (8)$$

$SOC(k+1)$, $SOC(k)$ are the SOC values of adjacent computation interval. ΔSOC is variation of SOC during each computation step, it is positive during charge, negative during discharge. T_{step} is computation step. T_{rating} is time for SOC from 0 to 100%. P_{rating} is rated power of the VRB.

C. *Model validation*

VRB is configured for basic block of BESS, rated power P_{rating}=5kW, rated capacity E_{capacity} =5kW×4h. Battery stack is composed with 39 battery cells in series, each battery cell normal EMF E=1.225V, maximum discharge current $I_{\max}$=95A, operation temperature T=298K. From the above data, it can be estimated that the equivalent parameters R_{reaction}=0.045Ω, $R_{\text{resistive}}$=0.03Ω, R_{fixed}=13.889Ω. If the measured battery cell capacity is 6F, then equivalent electrode capacitor for 39 battery cells in series $C_{\text{electrode}}$=6F/39=0.15F.

Charging the VRB continuously at a constant current of 95A for 2 hours, and then discharging the VRB at the same current for 2 hours. At a whole charge-discharge cycle, the simulation results are shown in Fig. 3.

According to the analysis of the above results: 1) I_{pump} is inversely proportional to *SOC*. In the charging process, with the increase of *SOC*, the flow rate of the pump is slowed down, and the I_{pump} is reduced. In the discharging process, with the decrease of *SOC*, the flow rate of the pump increases, and the I_{pump} increase accordingly; 2) with the change of *SOC*, the stack voltage of U_{stack} changes continuously, which reflects the concentration of vanadium in the electrolyte. In the charging process, U_{b} is greater than U_{stack}; In the discharging process, U_{b} is less than U_{stack}; 3) at the switching instant from charging to discharging, U_{b} is discontinuous due to the different current direction and voltage drop on the internal resistance. Moreover, during 0~20% SOC and 80~100% SOC, U_{b} and U_{stack} dramatically vary whether charging or discharging. However, VRB voltage is stable during 20~80% SOC, which provides a possibility for VRB to work in the range of 20~80% SOC in order to avoid over-charge or over-discharge in practical applications. The simulation results are in agreement with the VRB experimental characteristics in [14], which verify the correctness of the model.

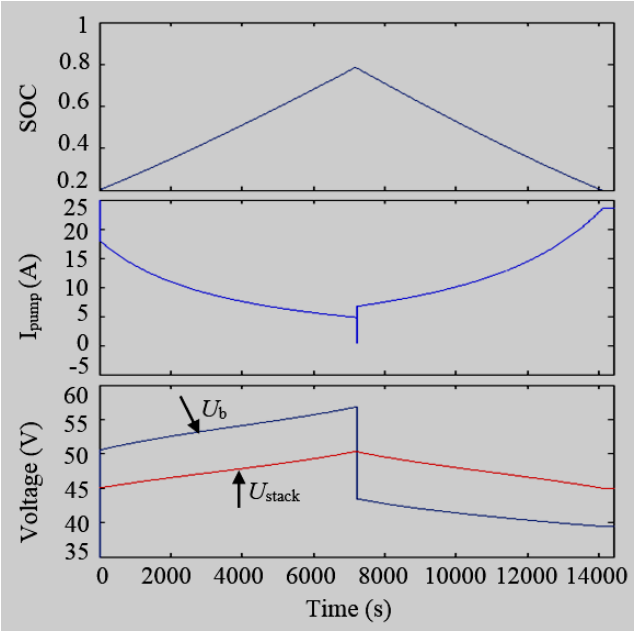

Figure 3. Simulation waveforms of VRB charge-discharge.

IV. OPERATION CHARACTERISTICS ANALYSIS OF VRB

A. *Constant current charge-discharge mode*

A charge-discharge experiment of 5kW/20kW·h battery system is carried out with constant current of 65A, 75A, 85A and 95A respectively, and the range of SOC is 20%~80%. Experimental results are shown in Fig. 4.

According to the results: 1) the stack voltage of different charge-discharge current is equal, but the response speed is different. Because the stack voltage U_{stack} depends only on the charge state SOC; 2) charge-discharge time is approximately proportional to the value of the current, and the charge time is slightly larger than the discharge time, which is caused by the parasitic loss of the VRB system and the loss of the pump; 3) the greater the constant charge discharge current I, the greater the difference between the terminal voltage U_b and the stack voltage U_{stack}. Because the greater the current, the greater the loss on the equivalent series resistance; 4) the input power P_b is greater than the absorption power of the battery pack P_s in the charging process, and the output power P_b is less than the release power of the battery pack P_s in the charging process. Because the equivalent loss in the charging process is provided by an external power supply, the battery is provided by the battery itself in the discharging process; 5) the greater the constant charge-discharge current, the greater the difference between the input-output power and the absorption-release power.

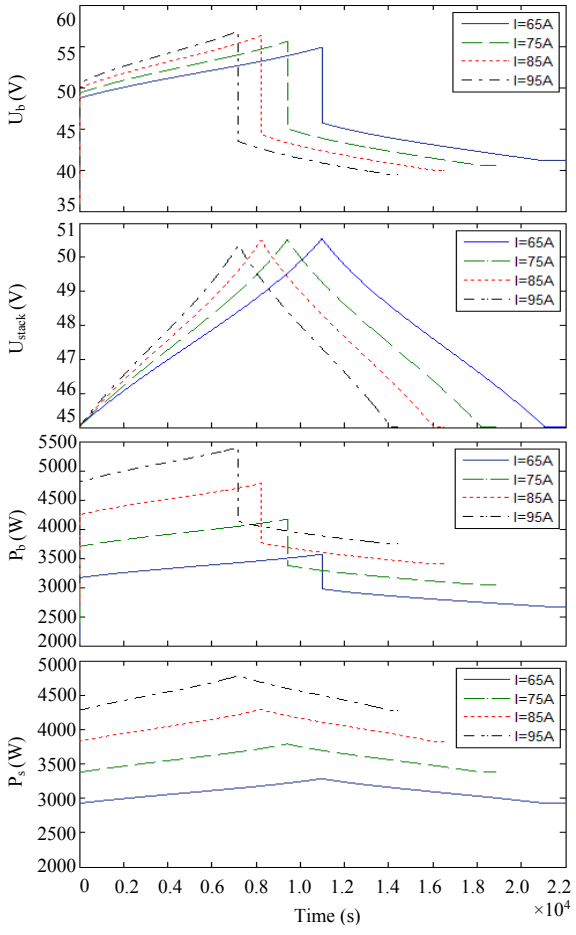

Figure 4. Simulation waveforms under constant current mode.

B. Constant power charge-discharge mode

A charge-discharge experiment of 5kW/20kW·h battery system is carried out with constant power of 3kW, 4kW, 5kW, 6kW and 7kW respectively, and the range of SOC is 20%~80%. Experimental results are shown in Fig. 5.

According to the results: 1) the greater the charge-discharge power P, the shorter the charge-discharge time; 2) the greater the constant charge-discharge power P, the greater the difference between the terminal voltage U_b and the stack voltage U_{stack}. Because the greater the current, the greater the loss on the equivalent series resistance; 3) VRB battery terminal input and output current I_b and the stack current I_s has a similar change law. The greater the charge-discharge power P, the greater the value of I_b and I_s. In the charging process, due to the increase of the battery terminal voltage, the current must be reduced to maintain constant power; In the discharging process, the battery terminal voltage U_b falling, in order to maintain constant power, the current must be increased to compensate for the voltage drop. 4) the input power P is greater than the absorption power of the battery pack P_s in the charging process, and the situation is the opposite in the discharging process.

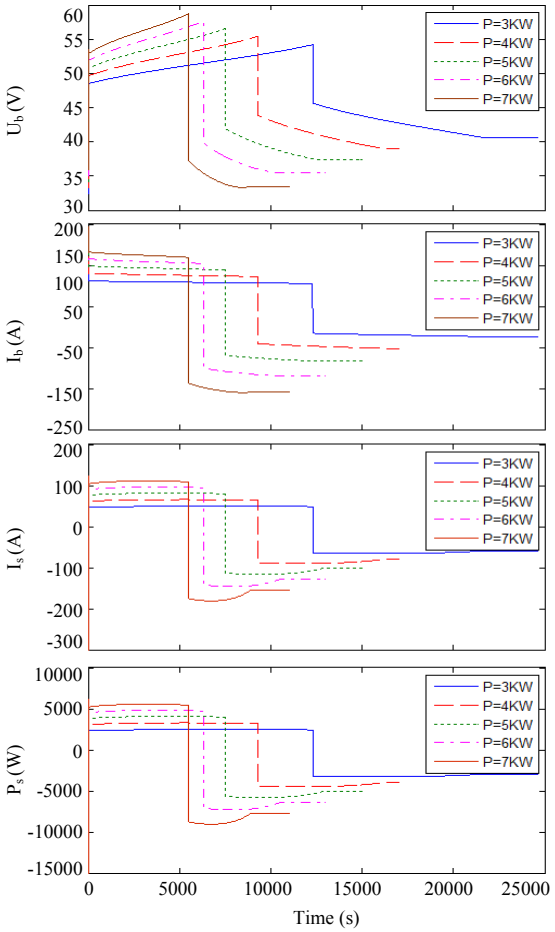

Figure 5. Simulation waveforms under constant power mode.

C. *Variable current charge-discharge mode*

Assuming that the charge current during 0~3000s is 65A, the charge current during 3000~7200s is 95A. The discharge current during 7200~10200s is 95A, the discharge current during 10200~14400s is 65A. The results are shown in Fig. 6.

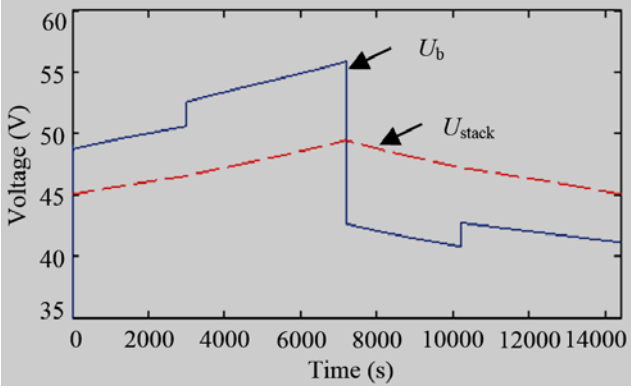

Figure 6. Simulation waveforms under variable current mode.

According to the analysis of the above results: when the charge current or discharge current mutate, the battery output voltage U_b will obviously mutate, and cell stack voltage U_{stack} only appear smaller non smooth change. In the rapid response of the charge and discharge process, the output voltage of the battery is a dramatic mutation according to the input and output current value. This characteristic presents higher requirements for the design of DC/DC bidirectional converter.

D. *VRB efficiency analysis*

The charge-discharge efficiency of the VRB is an important factor affecting the system efficiency. In the process of constant current charge-discharge, the battery efficiency is closely related to the charge-discharge current. Therefore, it is necessary to study the effect of charge-discharge current on the performance of the battery.

Coulomb efficiency is defined as

$$\eta_e = \frac{Q_2}{Q_1} \tag{9}$$

Charge efficiency is defined as

$$\eta_{charge} = \frac{E_{stack}}{E_{cell}} \tag{10}$$

Discharge efficiency is defined as

$$\eta_{discharge} = \frac{E_{cell}}{E_{stack}} \tag{11}$$

Q_1 and Q_2 are the charge and discharge capacity, E_{stack} and E_{cell} are the input and output energy of the battery.

Based on constant current charge-discharge experiment, the effect of different current on the efficiency of the VRB is obtained, the results are shown in Table 1.

TABLE I. VRB EFFICIENCY UNDER CCM

Current/A	Coulomb efficiency/%	Charge efficiency/%	Discharge efficiency/%
25	76.77	60.37	41.58
35	82.86	67.93	50.11
45	86.88	92.35	88.46
55	89.62	90.75	86.24
65	90.8	89.27	83.98
75	93.37	87.77	81.45
85	94.68	86.34	79.32
95	95.83	84.73	76.11

The fitting curves of the coulomb efficiency, charge efficiency and discharge efficiency can be obtained under different charge-discharge current, and the results are shown in Fig. 7.

According to the analysis of the above results: 1) the coulomb efficiency increases with the charge-discharge current. Because the higher the current, the shorter the charge discharge time, the smaller the self discharge capacity of the battery; 2) if the charge-discharge current is small, the charge-discharge efficiency increases with the current. When the current reaches a certain value, the polarization of the battery will increase, and the energy loss will increase sharply, which leads to the decrease of the battery charge-discharge efficiency.

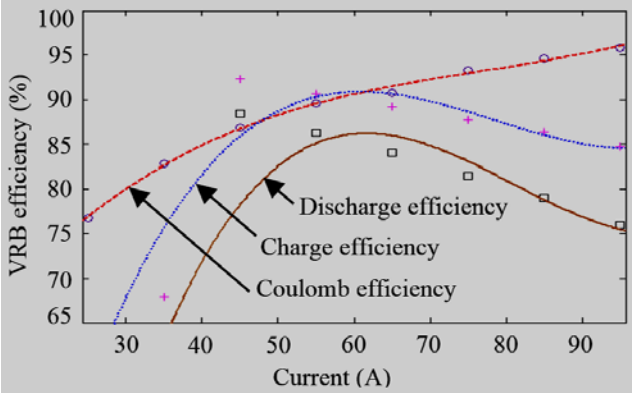

Figure 7. Simulation waveforms of VRB efficiency.

Based on the data of Table 1, the expression among the coulomb efficiency, the charging efficiency, the discharge efficiency and the charge-discharge current is as following:

$$\begin{cases} \eta_e = -0.0149I^2 + 1.294I + 52.92 \\ \eta_{charge} = 0.0003I^3 - 0.0684I^2 + 5.094I\text{-}31.04 \\ \eta_{discharge} = 0.0004I^3 - 0.0936I^2 + 7.149I - 89.06 \end{cases} \tag{12}$$

E. Transient characteristic analysis

Assuming that the charge current during 0~0.3s is 95A, and the VRB discharge with 95A current at 0.3s. The VRB charge again with 95A current at 0.4s. The output voltage of VRB is shown in Fig. 8.

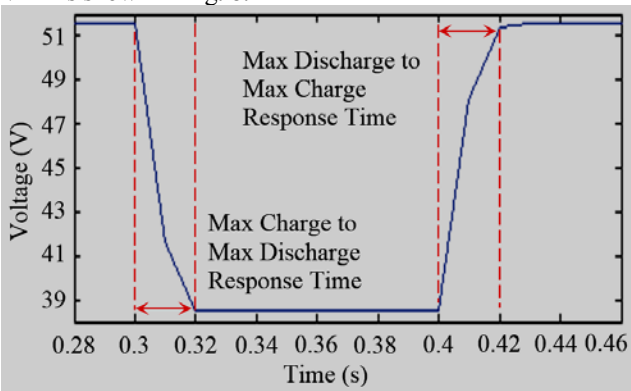

Figure 8. Transient characteristic of VRB.

According to the analysis of the above results, the transient characteristic of VRB is related to the concentration of the electrode and the electrolyte. During the process of state transition, the VRB need only about 20ms to reach the stable state, which reflect the excellent transient characteristic of VRB step response.

F. The effect of temperature on the stack voltage

The VRB is exothermic when it is running, and the heat transfer coefficient of the pipeline and the solution storage tank is small, so the measured temperature of the electrolyte is about 10 ℃ higher than the ambient temperature. Assuming that the VRB complete a charge-discharge cycle at a constant current of 95A, while the ambient temperature is -5℃, 25℃ and 35℃ respectively. The battery stack voltage varies with temperature is shown in Fig. 9.

According to the analysis of the above results: 1) the change of environmental temperature has no effect on the VRB constant current charge-discharge cycle; 2) the higher the ambient temperature, the higher the VRB stack voltage during the charge-discharge process, i.e., the higher the concentration of vanadium in the electrolyte. But when the electrolyte temperature is higher than 40℃, it is easy to decompose into V_2O_5 precipitation; Vanadium solution can precipitate out the crystal at low temperature. Two extremes of temperature can reduce the performance of the battery. The working temperature of the VRB can be set at 15~35℃, and the cooling system can be used to control and adjust the reaction temperature.

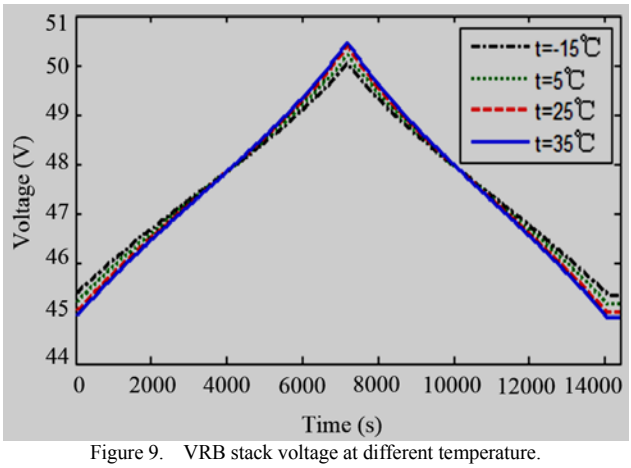

Figure 9. VRB stack voltage at different temperature.

V. CONCLUSION

The output characteristics and modeling complexity of the VRB model structure presented in this paper are taken into account. The model not only reflects SOC, internal loss and transient characteristics of VRB, but also is convenient for simulation and engineering realization. The mathematical model between VRB battery efficiency and charge-discharge current is put forward for the first time, and the effects of transient features and temperature on the battery performance are analyzed. The work done in this paper lays the good theoretical foundation for further study of the VRB energy storage system.

ACKNOWLEDGMENT

This work was supported by National Natural Science Foundation of China (51267015) and Specialized Research Fund for the Doctoral Program of Higher Education of China (20121514110005).

REFERENCES

[1] Dong Weijie, Bai Xiaomin, and Zhu Ninghui, "Discussion on the power quality under grid-connection of intermittent power sources", Power System Technology, vol. 37, No. 5, pp.1265-1271, 2013.

[2] Wang Yanling, Zhang Xuejiao, and Yan Jingmin, "Weight-varying gray cloud model based comprehensive evaluation on technical performance of overall grid-integration of wind farm", Power System Technology, vol. 37, No. 12, pp.3546-3551, 2013.

[3] He Shien, Yao Xu, and Xu Shanfei, "Impacts of large-scale wind power integration on relay protection and countermeasures", Power System Protection and Control, vol. 41, No. 1, pp.21-27, 2013.

[4] Hamidi V, Li Furong, and Yao Liangzhong, "Value of wind power at different locations in the grid", IEEE Transactions on Power Delivery, vol. 26, No. 2, pp.526-537, 2011.

[5] Dunn B, KAMATH H, and TARASCON J M, "Electrical energy storage for the grid: a battery of choices", Science, vol. 334, No. 6058, pp.928-935, 2011.

[6] Ding Ming, Wu Jianfeng, and Zhu Chengzhi, "A real-time smoothing control strategy with soc adjustment function of storage systems", Proceedings of the CSEE, vol. 33, No. 1, pp.22-29, 2013.

[7] Yang Z, Zhang J, and MC K M, "Electrochemical energy storage for green grid", Chemical Review, vol. 111, No. 5, pp.3577-3613, 2013.

[8] Luo Xing, Wang Jihong, and Ma Zhao, "Overview of energy storage technologies and their application prospects in smart grid", Smart Grid, vol. 2, No. 1, pp.7-12, 2014.
[9] Wang Yufei, Fu Yang, and Zhang Yu, "Characteristics analysis and experimental study of wind power energy storage systems", Acta Energiae Solaris Sinica, vol. 31, No. 11, pp.1510-1515,2010.
[10] Chen Jinqing, Zhu Shunquan, and Wang Baoguo, "Model of open-circuit viltage for all-vanadium redox flow battery", CIESC Journal, vol. 60, No. 1, pp.211-215, 2009.
[11] Li Guojie, Tang Zhiwei, and Nie Hongzhan, "Modelling and controlling of vanadium redox flow battery to smooth wind power fluctuations", Power System Protection and Control, vol. 38, No. 22, pp.115-120, 2010.
[12] Shah A A, Watt-Smith M J, "A dynamic performance model for redox flow batteries involving soluble species", Electrochemical Acta, vol. 53, No. 27, pp.8087-8100, 2008.
[13] Yang Linlin, Liao Wenjun, and Su Qing, "The research and development status of vanadium redox flow battery", Energy Storage Science and Technology, vol. 2, No. 2, pp.140-145, 2013.
[14] Zhao Ping, Zhang Huamin, and Wen Yuehua, "Charge-discharge behaviors and properties of a lab-scale all-vanadium redox-flow single cell", Electrochemistry, vol. 13, No. 1, pp.12-18, 2007.